

The quantum *vs* classical aspects of one dimensional electron-phonon systems revisited by the renormalization group method

H. Bakrim and C. Bourbonnais

*Regroupement Québécois sur les Matériaux de Pointe, Département de physique,
Université de Sherbrooke, Sherbrooke, Québec, Canada, J1K-2R1*

(Dated:)

An extension of the renormalization group method that includes the effect of retardation for the interactions of a fermion gas is used to re-examine the quantum and classical properties of Peierls-like states in one dimension. For models of spinless and spin- $\frac{1}{2}$ fermions interacting with either intra or intermolecular phonons the quantum corrections to the Peierls gap at half-filling are determined at arbitrary phonon frequency. The nature of quantum-classical transitions is clarified in weak coupling.

PACS numbers: 71.10.Pm, 71.10.Hf, 63.20.Kr, 05.10.Cc

I. INTRODUCTION

The influence exerted by zero point ionic motion on the stability of the Peierls and spin-Peierls lattice distorted states enters as a key ingredient in the elaboration of a general theoretical description of these phases. Quantum fluctuations are known to cause a downward renormalization of the order parameter and the corresponding electronic gap, if not their complete suppression as it is the case for spin-Peierls order. One is confronted to such situations in low dimensional conductors and insulators for which the characteristic phonon energy is not only finite in practice, but may exceed by far the temperature scale at which the lattice instability takes place. These cases are exemplified in spin-Peierls systems like the inorganic compound CuGeO_3 ,^{1,2} the organic system $\text{MEM}(\text{TCNQ})_2$,² and also members of the $(\text{TMTTF})_2\text{X}$ series of organic compounds for which non adiabaticity emerges as one moves along the pressure scale, giving rise to quantum criticality for the spin-Peierls transition.³

The first systematic studies of quantum effects on the Peierls-type distorted states go back in the eighties with the world-line Monte Carlo simulations of Hirsch and Fradkin.^{4,5} These simulations were made on the one-dimensional tight binding and Holstein electron-phonon models, also known as the Su-Schrieffer-Heeger (SSH)⁶ and the molecular crystal (MC)⁷ models. The stability of lattice distorted phases was determined as a function of the ionic mass and the strength of electron-phonon coupling. The phase diagrams of the models were outlined for both spinless and spin- $\frac{1}{2}$ fermions at half-filling. These initial works were followed by a variety of numerical techniques applied to the same models and extended to include direct interactions between fermions. That is how density matrix renormalization group (DMRG),^{8,9,10} exact diagonalizations,¹¹ and quantum Monte Carlo¹² techniques to mention a few, have contributed to provide a fairly coherent picture of the influence wielded by zero point lattice fluctuations in one-dimensional electron-phonon systems.

On the analytical side, these progress were

preceded^{13,14} and accompanied^{4,5,15,16,17,18,19,20} by a whole host of approaches applied to study retardation effects on lattice distortion at intermediate phonon frequencies. The renormalization group (RG) method^{15,17,18,21,22} has been one of the routes proposed to deal with this problem. A variant of the RG method will be further developed in this work. Our analysis starts with the effective fermionic formulation of the electron-phonon problem, which is expressed in terms of a fermion gas in the continuum with weak retarded interactions. Such a formulation for the SSH and MC models has been investigated long ago by the two-cutoff scaling method.¹⁵ In this approach the characteristic bandwidth energy E_0 for fermions and the vibrational energy ω_c ($\hbar = 1$) for phonons determine the form of flow equations for the electronic scattering amplitudes,¹⁴ whose singularities signal the creation of gaps and long-range order at half-filling. Thus when the electronic mean-field energy gap Δ_0 – emerging below E_0 in the adiabatic weak coupling theory – is larger than ω_c , quantum corrections are neglected and the flow is equivalent to a ladder diagrammatic summation compatible with the unrenormalized static scale Δ_0 for the gap. On the other hand when $\Delta_0 < \omega_c$, the scattering amplitudes, though still governed by the ladder flow down to ω_c , are considered as effective unretarded interactions at lower energies. Below ω_c the flow becomes impregnated by vertex corrections and interference between different scattering channels. In accord with the well known results of the one-dimensional electron gas model,^{23,24,25,26} the classical gap Δ_0 is then an irrelevant scale and the system enters in the non adiabatic quantum domain where either a gapless or an ordered massive phase can occur.

While the two-cutoff RG analysis can provide a simple and reliable criteria to map out the essentials of the quantum-classical boundaries of the phase diagram for both models in the weak coupling sector,^{8,9} it says nothing, on the other hand, on how the gap varies over the whole phonon frequency range. This is not only of practical importance, when *e.g.*, the theory is confronted to experiment in concrete cases, but also clearly

needed on general grounds when one raises the question of the nature of quantum-classical transition as a function of phonon frequency. This drawback is not a weakness of the RG method in general but rather ensues from the frequency dependence of couplings, which in the two cut-off scaling approach, barely reduces to the minimum found in either the adiabatic or non adiabatic limit. A continuous description of retardation effects would require that the full functional dependence of scattering amplitudes on the frequencies be restored, a possibility that can be likened to what has been done in two-dimensional and quasi-one-dimensional RG for the functional dependence on scattering amplitudes on the momentum.^{27,28,29,30,31,32} Very recent progress along these lines show that it is indeed a promising avenue.³³

In this paper we shall revert to the RG approach as developed in Refs.^{26,34} and extend its formulation to include the frequency dependence of scattering amplitudes introduced by the electron-phonon interaction. We revisit the classical and quantum aspects of fermion driven lattice instabilities. Our analysis is done at the one-loop level and covers the gap determination and the structure of the phase diagram of the MC and SSH models for both spinless and spin- $\frac{1}{2}$ fermions. Although the generalization to incommensurate band filling and situations where the direct Coulomb interaction is included would cause no difficulty, we have restricted our analysis to retarded interactions at half-filling. In Sec. II, we introduce the electron-phonon models and recall the derivation of their respective bare retarded interactions in the framework of an effective fermion gas model. We pay special attention to the SSH model in the spinless case in order to include the momentum dependent umklapp term to the interaction parameter space, which is so important for long-range order of this model. In Sec. III the one-loop level flow equations for the retarded scattering amplitudes and response functions are derived for spinless and spin- $\frac{1}{2}$ fermions. In Sec. IV we compute the variations of the gap over the whole frequency range and discuss the structure of the phase diagram and the nature of the quantum-classical transitions for the MC and SSH models. We conclude in Sec. V.

II. THE MODELS AND THE PARTITION FUNCTION

A. Models

The one-dimensional electron-phonon models that we shall study using the RG method are the MC and the

SSH models. The MC model describes the coupling of fermions to optical molecular phonon modes, whereas for the SSH model the electron-phonon interaction results from the modulation of electronic energy by acoustic phonons. In Fourier space, the two one-dimensional models Hamiltonians can be written in following form

$$\begin{aligned} H &= H_0 + H_{\text{ph}} + H_{\text{I}} \\ &= \sum_{k,\sigma} \epsilon(k) c_{k,\sigma}^\dagger c_{k,\sigma} + \sum_q \omega_q \left(b_q^\dagger b_q + \frac{1}{2} \right) \\ &\quad + L^{-\frac{1}{2}} \sum_{k,q,\sigma} g(k,q) c_{k+q,\sigma}^\dagger c_{k,\sigma} (b_q^\dagger + b_{-q}). \end{aligned} \quad (1)$$

Here H_0 is the free fermion part and $\epsilon(k) = -2t \cos k$ is the tight-binding energy spectrum with t as the hopping integral (the lattice constant $a = 1$ and L is the number of sites). $c_{k,\sigma}^\dagger$ ($c_{k,\sigma}$) creates (annihilates) a fermion of wave vector k and spin σ . H_{ph} and H_{I} terms correspond to the free phonon and electron-phonon interaction parts, respectively, and in which b_q^\dagger (b_q) creates (annihilates) a phonon of wave vector q . For the MC model,⁷ the intramolecular phonon energy and the interaction are given by

$$\omega_q = \omega_0, \quad (2)$$

$$g(k,q) = \lambda_0 / \sqrt{2M_0\omega_0}, \quad (3)$$

which are both independent of the momentum. Here $\lambda_0 > 0$ is the amplitude of the electron-phonon interaction on each molecular site whereas the frequency $\omega_0 = \sqrt{\kappa_0/M_0}$ is expressed in terms of the elastic constant κ_0 and the molecular mass M_0 .

For the SSH model,⁶ the corresponding quantities read

$$\omega_q = \omega_D \left| \sin \frac{q}{2} \right|, \quad (4)$$

$$g(k,q) = i4 \frac{\lambda_D}{\sqrt{2M_D\omega_D}} \sin \frac{q}{2} \cos \left(k + \frac{q}{2} \right), \quad (5)$$

where $\omega_D = 2\sqrt{\kappa_D/M_D}$ is the acoustic phonon energy at $q = 2k_F$, namely at twice the Fermi wave vector $k_F = \pi/2$ at half-filling. M_D is the ionic mass and κ_D is the constant force of the one-dimensional lattice.

B. The partition function

Following the trace over harmonic phonon degrees of freedom in the interaction Matsubara time representation of the grand canonical partition function Z , one can write

$$Z = \text{Tr}_e e^{-\beta H_0 - \mu N} \text{Tr}_{\text{ph}} e^{-\beta H_{\text{ph}}} T_\tau \exp \left\{ - \int_0^\beta H_{\text{I}}(\tau) d\tau \right\}$$

$$= Z_{\text{ph}} \text{Tr}_e e^{-\beta H_0 - \mu N} T_\tau \exp \left\{ -\frac{1}{2} \sum_{\{k,q,\sigma\}} \int_0^\beta \int_0^\beta g(k,q) g(k',-q) D(q, \tau - \tau') c_{k+q,\sigma}^\dagger(\tau) c_{k'-q,\sigma'}^\dagger(\tau') c_{k',\sigma'}(\tau') c_{k,\sigma}(\tau) d\tau' d\tau \right\} \quad (6)$$

where Z_{ph} is the partition function of bare phonons. The phonon integration introduces an effective ‘retarded’ fermion interaction mediated by phonons and described by the bare propagator

$$D(q, \tau - \tau') = e^{-\omega_q |\tau - \tau'|} + 2(e^{\beta \omega_q} - 1)^{-1} \cosh(\omega_q(\tau - \tau')).$$

The remaining trace over fermion degrees of freedom can be recast into a functional integral form

$$\begin{aligned} Z &= Z_{\text{ph}} \iint \mathcal{D}\psi^* \mathcal{D}\psi e^{S[\psi^*, \psi]}, \\ &= Z_{\text{ph}} \iint \mathcal{D}\psi^* \mathcal{D}\psi e^{S_0[\psi^*, \psi] + S_I[\psi^*, \psi]}, \end{aligned} \quad (7)$$

over the anticommuting Grassman fields ψ . In the Fourier Matsubara space, the free fermionic action is

$$S_0[\psi^*, \psi] = \sum_{p, \tilde{k}, \sigma} [G_p^0(\tilde{k})]^{-1} \psi_{p,\sigma}^*(\tilde{k}) \psi_{p,\sigma}(\tilde{k}), \quad (8)$$

where

$$G_p^0(\tilde{k}) = [i\omega - \epsilon_p(k)]^{-1} \quad (9)$$

is the bare fermion propagator for $\tilde{k} = (k, \omega = \pm\pi T, \pm 3\pi T, \dots)$ ($k_B = 1$). The fermion spectrum $\epsilon(k) - \mu \approx \epsilon_p(k) = v_F(pk - k_F)$ is linearized around the right ($p = +$) and left ($p = -$) Fermi points $\pm k_F$. The bandwidth cut-off $E_0 = 2E_F$ is twice the Fermi energy $E_F = v_F k_F$. The integration of the fermion degrees of freedom becomes $\iint \mathcal{D}\psi^* \mathcal{D}\psi = \iint \prod_{p,\sigma,\tilde{k}} d\psi_{p\sigma}^*(\tilde{k}) d\psi_{p\sigma}(\tilde{k})$.

The interacting part S_I of the action reads

$$S_I[\psi^*, \psi] = -\frac{T}{2L} \sum_{\{p,\tilde{k},\sigma\}} g(\tilde{k}_1, \tilde{k}_2; \tilde{k}_3, \tilde{k}_4) \psi_{p_1,\sigma_1}^*(\tilde{k}_1) \psi_{p_2,\sigma_2}^*(\tilde{k}_2) \psi_{p_4,\sigma_2}(\tilde{k}_4) \psi_{p_3,\sigma_1}(\tilde{k}_3) \delta_{k_{1+2}, k_{3+4} + G} \delta_{\omega_{1+2}, \omega_{3+4}}, \quad (10)$$

where momentum conservation is assured modulo the reciprocal lattice vector $G = \pm 4k_F$, allowing for umklapp scattering at half-filling. In the Fourier-Matsubara space, the interaction takes the form

$$g(\tilde{k}_1, \tilde{k}_2; \tilde{k}_3, \tilde{k}_4) = g(k_1, k_3 - k_1) g(k_2, k_4 - k_2) D(\tilde{k}_3 - \tilde{k}_1), \quad (11)$$

where

$$D(\tilde{k}_3 - \tilde{k}_1) = -2 \frac{\omega_{k_3 - k_1}}{\omega_{k_3 - k_1}^2 + \omega_{3-1}^2},$$

is the bare phonon propagator. We can now proceed to the ‘g-ology’ decomposition of this interaction. This will be done separately for fermions with and without spins.

In the first place, for spin- $\frac{1}{2}$ fermions, we shall consider the three standard couplings between fermions on opposite Fermi points

$$g_1(\omega_1, \omega_2, \omega_3) \equiv g(\pm k_F, \omega_1, \mp k_F, \omega_2; \mp k_F, \omega_3, \pm k_F, \omega_4),$$

$$g_2(\omega_1, \omega_2, \omega_3) \equiv g(\pm k_F, \omega_1, \mp k_F, \omega_2; \pm k_F, \omega_3, \mp k_F, \omega_4),$$

$$g_3(\omega_1, \omega_2, \omega_3) \equiv g(\pm k_F, \omega_1, \pm k_F, \omega_2; \mp k_F, \omega_3, \mp k_F, \omega_4),$$

$$(12)$$

for retarded backward, forward and umklapp scattering amplitudes, respectively (here the forward scattering of fermions on the same branch is neglected). According to Eq. (3), the bare frequency dependent couplings for the MC model become

$$g_{i=1,2,3}(\omega_1, \omega_2, \omega_3) = \frac{g_i}{1 + \omega_{3-1}^2 / \omega_0^2}, \quad (13)$$

where $g_{i=1,2,3} = -\lambda_0^2 / \kappa_0$ is the (M_0 -independent) attractive amplitude. Similarly for the SSH model, one has from Eq. (5)

$$g_{1,3}(\omega_1, \omega_2, \omega_3) = \frac{g_{1,3}}{1 + \omega_{3-1}^2 / \omega_D^2}, \quad (14)$$

where the amplitudes $g_{1,3} = \mp 4\lambda_D^2 / \kappa_D$ are also M_D -independent. For the SSH model, the bare forward scattering amplitude g_2 vanishes for the exchange of zero momentum phonon but it will be generated at lower energy by the renormalization group transformation.

For spinless fermions, the backward scattering is indistinguishable by exchange from the forward scattering

and both can be combined to define an effective forward scattering term of the form

$$\begin{aligned} g_f(\omega_1, \omega_2, \omega_3) &\equiv g(\pm k_F, \omega_1, \mp k_F, \omega_2; \pm k_F, \omega_3, \mp k_F, \omega_4) \\ &- g(\pm k_F, \omega_2, \mp k_F, \omega_1; \mp k_F, \omega_3, \pm k_F, \omega_4) \\ &= \frac{g_2}{1 + \omega_{3-1}^2/\omega_{0,D}^2} - \frac{g_1}{1 + \omega_{3-2}^2/\omega_{0,D}^2}, \end{aligned} \quad (15)$$

where the mass independent amplitudes are $g_{1,2} = -\lambda_0^2/\kappa_0$ for the MC model, and $g_1 = -4\lambda_D^2/\kappa_D$ and $g_2 = 0$ in the SSH case.

As for the umklapp scattering in the spinless case, it must be antisymmetrized with its own exchange term to give the following two contributions

$$\begin{aligned} \frac{1}{2}[g(\tilde{k}_1, \tilde{k}_2; \tilde{k}_3, \tilde{k}_4) - g(\tilde{k}_2, \tilde{k}_1; \tilde{k}_3, \tilde{k}_4)]_{k_1 \sim k_2}^{k_3 \sim k_4} &\equiv g_3(\omega_1, \omega_2, \omega_3) \\ &+ g_u(\omega_1, \omega_2, \omega_3)(\sin k_1 - \sin k_2)(\sin k_3 - \sin k_4). \end{aligned} \quad (16)$$

The first contribution corresponds to a local umklapp term defined for incoming and outgoing fermions *at* the Fermi points. It takes the form

$$\begin{aligned} g_3(\omega_1, \omega_2, \omega_3) &= \frac{1}{2}[g(\pm k_F, \omega_1, \pm k_F, \omega_2; \mp k_F, \omega_3, \mp k_F, \omega_4) \\ &- g(\pm k_F, \omega_2, \pm k_F, \omega_1; \mp k_F, \omega_3, \mp k_F, \omega_4)] \\ &= \frac{g_3}{1 + \omega_{3-1}^2/\omega_{0,D}^2} - \frac{g_3}{1 + \omega_{3-2}^2/\omega_{0,D}^2}, \end{aligned} \quad (17)$$

This term is present for both models, where $g_3 = -\lambda_0^2/\kappa_0$ is attractive for the MC model, and $g_3 = 4\lambda_D^2/\kappa_D$ is repulsive for the SSH model. The second term of (16) is a non local – momentum dependent – umklapp contribution and is only present for the SSH model. Actually this additional contribution follows from the antisymmetrization of Eq. (11) and the use of (5) under the permutation of incoming and outgoing frequencies and momentum (these last, *not* at the Fermi points). Its frequency dependent part reads

$$g_u(\omega_1, \omega_2, \omega_3) = g_u \left[\frac{1}{1 + \omega_{3-1}^2/\omega_D^2} + \frac{1}{1 + \omega_{3-2}^2/\omega_D^2} \right], \quad (18)$$

where the amplitude is given by $g_u = \lambda_D^2/2\kappa_D$. From Eq. (16), it follows that for $k_{1(3)} \sim k_{2(4)}$, the leading k -dependence of the non local umklapp is $\propto (k_1 - k_2)(k_3 - k_4)$ which has a scaling dimension of -2. This term is therefore strongly irrelevant at the tree level but becomes relevant beyond some threshold in the electron-phonon interaction. Such umklapp contributions are well known to play a key role in the existence of long-range order for interacting spinless fermions,^{35,36} as it will show to be the case for the SSH model.^{4,8,15}

III. THE RENORMALIZATION GROUP TRANSFORMATION

The renormalization group transformation for the partition function will follow the one given in Ref.^{26,34} One

then proceeds for Z to the successive partial integration of fermion degrees of freedom, denoted by $\bar{\psi}^{(*)}$ having the momentum located in the outer energy shells (o.s) $\pm E_0(\ell)d\ell/2$ above and below the Fermi points for each fermion branch p . The remaining ($<$) degrees of freedom are kept fixed. Here $E_0(\ell) = E_0 e^{-\ell}$ is the scaled bandwidth at $\ell \geq 0$. The integration proceeds by first splitting the action $S \rightarrow S[\psi^*, \bar{\psi}]_\ell + \bar{S}_0 + \bar{S}_I$ into an inner shell part at ℓ and the $\bar{\psi}$ – dependent outer shell terms \bar{S}_0 and \bar{S}_I . Considering \bar{S}_I as a perturbation with respect to the free outer-shell action \bar{S}_0 , the partial integration at the one-loop level is of the form

$$\begin{aligned} Z &\sim \iint_{<} \mathcal{D}\psi^* \mathcal{D}\psi e^{S[\psi^*, \psi]_\ell} \\ &\times \iint_{\text{o.s}} \mathcal{D}\bar{\psi}^* \mathcal{D}\bar{\psi} e^{\bar{S}_0[\bar{\psi}^*, \bar{\psi}] + \bar{S}_I[\bar{\psi}^*, \bar{\psi}, \psi^*, \psi]} \\ &\propto \iint_{<} \mathcal{D}\psi^* \mathcal{D}\psi e^{S[\psi^*, \psi]_\ell + \langle \bar{S}_I \rangle_{\text{o.s}} + \frac{1}{2} \langle \bar{S}_I^2 \rangle_{\text{o.s}} + \dots} \end{aligned} \quad (19)$$

Here the interacting part is made up of three pertinent terms, *i.e.*, $\bar{S}_I = \bar{S}_{I,2}^P + \bar{S}_{I,2}^C + \bar{S}_{I,2}^L$, for all possibilities of putting simultaneously two outer shell fields in the $2k_F$ electron-hole Peierls channel ($\bar{S}_{I,2}^P \sim \bar{\psi}_+^* \psi_-^* \bar{\psi}_- \psi_+ + \bar{\psi}_+^* \psi_+^* \bar{\psi}_- \psi_- + \dots$), the zero momentum fermion-fermion Cooper channel ($\bar{S}_{I,2}^C \sim \bar{\psi}_+^* \bar{\psi}_-^* \psi_- \psi_+ + \dots$), and the Landau channel ($\bar{S}_{I,2}^L \sim \bar{\psi}_+^* \bar{\psi}_-^* \bar{\psi}_- \psi_+ + \dots$).

The lowest order outer shell statistical average $\langle \bar{S}_I \rangle_{\text{o.s}}$ comes from the Landau part and gives rise to the self-energy corrections $\delta\Sigma(\omega)$ of the one-particle Green function, which becomes $G_p^{-1} + i\delta\Sigma(\omega)$. As for the contractions $\frac{1}{2} \langle \bar{S}_I^2 \rangle_{\text{o.s}}$, only the singular Peierls and Cooper scattering channels are retained; with four fields in the inner shell, these correspond to corrections to the coupling constants. Both corrections define the renormalized action $S[\psi^*, \bar{\psi}]_{\ell+d\ell}$ at the step $\ell + d\ell$.

The evaluation of outer shell contractions $\langle \bar{S}_I \rangle_{\text{o.s}}$ for the self-energy at the one-loop level leads to

$$\begin{aligned} \langle \bar{S}_I \rangle_{\text{o.s}} &= i\delta\Sigma(\omega) \sum_{p, \tilde{k} < \sigma} \psi_{p,\sigma}^*(\tilde{k}) \psi_{p,\sigma}(\tilde{k}), \\ \delta\Sigma(\omega) &= -\pi v_F \frac{T}{L} \sum_{\omega'} \sum_{\{k\}_{\text{o.s}}} \tilde{g}_s(\omega', \omega, \omega) G_-(k, \omega'). \end{aligned} \quad (20)$$

In the low temperature limit, the flow equation for the self-energy becomes

$$\begin{aligned} \partial_\ell \Sigma(\omega) &= \int_{-\infty}^{+\infty} \frac{d\omega'}{2\pi} \left\{ \tilde{g}_s(\omega', \omega, \omega) \right. \\ &\times \left. \frac{(E_0(\ell)/2)(\omega' - \Sigma(\omega'))}{(\omega' - \Sigma_p(\omega'))^2 + (E_0(\ell)/2)^2} \right\}, \end{aligned} \quad (21)$$

where

$$\tilde{g}_s(\omega', \omega, \omega) = \tilde{g}_1(\omega', \omega, \omega) - 2\tilde{g}_2(\omega, \omega', \omega), \quad (22)$$

for spin- $\frac{1}{2}$ fermions, and

$$\tilde{g}_s(\omega', \omega, \omega) = -\tilde{g}_f(\omega, \omega', \omega), \quad (23)$$

in the spinless case. Here $\tilde{g}_i(\{\omega\}) \equiv g_i(\{\omega\})/\pi v_F$, $\partial_\ell \equiv \partial/\partial\ell$, and $\Sigma(\omega) = 0$ at $\ell = 0$.

$[\frac{1}{2}\langle(S_{I,2}^P)^2\rangle_{\text{o.s.}}]$ and Cooper $[\frac{1}{2}\langle(S_{I,2}^C)^2\rangle_{\text{o.s.}}]$ channels. For the MC and SSH models defined by the initial couplings (13-14), these interfering contractions lead to the flow equations

A. RG flow for couplings: spin- $\frac{1}{2}$ fermions

The one-loop contractions $\frac{1}{2}\langle\bar{S}_I^2\rangle_{\text{o.s.}}$ amount to evaluate the outer shell contributions of the Peierls

$$\begin{aligned} \partial_\ell \tilde{g}_1(\omega_1, \omega_2, \omega_3) = \int_{-\infty}^{+\infty} \frac{d\omega}{2\pi} \{ & - 2 \tilde{g}_1(\omega, \omega_2, \omega + \omega_3 - \omega_1) \tilde{g}_1(\omega_1, \omega + \omega_3 - \omega_1, \omega_3) I_P(\omega, \omega_3 - \omega_1) \\ & + \tilde{g}_1(\omega, \omega_2, \omega + \omega_3 - \omega_1) \tilde{g}_2(\omega + \omega_3 - \omega_1, \omega_1, \omega_3) I_P(\omega, \omega_3 - \omega_1) \\ & + \tilde{g}_1(\omega_1, \omega, \omega_3) \tilde{g}_2(\omega_2, \omega + \omega_1 - \omega_3, \omega) I_P(\omega, \omega_1 - \omega_3) \\ & - 2 \tilde{g}_3(\omega_2, \omega, \omega_1 + \omega_2 - \omega_3) \tilde{g}_3(\omega_1, \omega + \omega_3 - \omega_1, \omega_3) I_P(\omega, \omega_3 - \omega_1) \\ & + \tilde{g}_3(\omega_1, \omega, \omega_3) \tilde{g}_3(\omega + \omega_1 - \omega_3, \omega_2, \omega_1 + \omega_2 - \omega_3) I_P(\omega, \omega_1 - \omega_3) \\ & + \tilde{g}_3(\omega_2, \omega, \omega_1 + \omega_2 - \omega_3) \tilde{g}_3(\omega + \omega_3 - \omega_1, \omega_1, \omega_3) I_P(\omega, \omega_3 - \omega_1) \\ & - \left[\tilde{g}_2(\omega_2, \omega_1, \omega + \omega_1 + \omega_2) \tilde{g}_1(-\omega, \omega_2, \omega_1 + \omega_2 + \omega) \right. \\ & \left. + \tilde{g}_1(\omega_1, \omega_2, \omega + \omega_1 + \omega_2) \tilde{g}_2(\omega + \omega_1 + \omega_2, -\omega, \omega_3) \right] I_C(\omega, \omega_1 + \omega_2) \} \end{aligned} \quad (24)$$

$$\begin{aligned} \partial_\ell \tilde{g}_2(\omega_1, \omega_2, \omega_3) = \int_{-\infty}^{+\infty} \frac{d\omega}{2\pi} \{ & \left[\tilde{g}_2(\omega_1, \omega + \omega_2 - \omega_3, \omega) \tilde{g}_2(\omega, \omega_2, \omega_3) \right. \\ & \left. + \tilde{g}_3(\omega_1, \omega + \omega_2 - \omega_3, \omega) \tilde{g}_3(\omega, \omega_2, \omega_3) \right] I_P(\omega, \omega_2 - \omega_3) \\ & - \left[\tilde{g}_2(\omega_1, \omega_2, \omega + \omega_1 + \omega_2) \tilde{g}_2(\omega + \omega_1 + \omega_2, -\omega, \omega_3) \right. \\ & \left. + \tilde{g}_1(\omega_2, \omega_1, \omega + \omega_1 + \omega_2) \tilde{g}_1(-\omega, \omega + \omega_1 + \omega_2, \omega_3) \right] I_C(\omega, \omega_1 + \omega_2) \} \end{aligned} \quad (25)$$

$$\begin{aligned} \partial_\ell \tilde{g}_3(\omega_1, \omega_2, \omega_3) = 2 \int_{-\infty}^{+\infty} \frac{d\omega}{2\pi} \{ & - 2 \tilde{g}_1(\omega_1, \omega + \omega_3 - \omega_1, \omega_3) \tilde{g}_3(\omega, \omega_2, \omega + \omega_3 - \omega_1) I_P(\omega, \omega_3 - \omega_1) \\ & + \tilde{g}_1(\omega_1, \omega, \omega_3) \tilde{g}_3(\omega + \omega_1 - \omega_3, \omega_2, \omega_1 + \omega_2 - \omega_3) I_P(\omega, \omega_1 - \omega_3) \\ & + \tilde{g}_3(\omega_1, \omega, \omega_3) \tilde{g}_2(\omega + \omega_1 - \omega_3, \omega_2, \omega_1 + \omega_2 - \omega_3) I_P(\omega, \omega_1 - \omega_3) \\ & + \tilde{g}_3(\omega, \omega_2, \omega_3) \tilde{g}_2(\omega + \omega_2 - \omega_3, \omega_1, \omega_1 + \omega_2 - \omega_3) I_P(\omega, \omega_2 - \omega_3) \}. \end{aligned} \quad (26)$$

The momentum shell Peierls and Cooper loops $I_P(\omega, \Omega)$ and $I_C(\omega, \Omega)$ at internal ω and their respective external

frequency Ω are by using the Green function with self-energy corrections

$$\begin{aligned}
I_P(\omega, \Omega) d\ell &= -\frac{\pi v_F}{L} \sum_{\{k\}_{\text{o.s.}}} G_+(k + 2k_F, \omega + \Omega) G_-(k, \omega), \\
&= \frac{d\ell}{2} E_0(\ell) \frac{(\omega - \Sigma(\omega))(\omega + \Omega - \Sigma(\omega + \Omega)) + \frac{1}{4} E_0^2(\ell)}{[(\omega - \Sigma(\omega))^2 + \frac{1}{4} E_0^2(\ell)][(\omega + \Omega - \Sigma(\omega + \Omega))^2 + \frac{1}{4} E_0^2(\ell)]},
\end{aligned} \tag{27}$$

$$\begin{aligned}
I_C(\omega, \Omega) d\ell &= \frac{\pi v_F}{L} \sum_{\{k\}_{\text{o.s.}}} G_+(k, \omega + \Omega) G_-(-k, -\omega), \\
&= \frac{d\ell}{2} E_0(\ell) \frac{(\omega - \Sigma(\omega))(\omega - \Omega + \Sigma(\Omega - \omega)) + \frac{1}{4} E_0^2(\ell)}{[(\omega - \Sigma(\omega))^2 + \frac{1}{4} E_0^2(\ell)][(\omega - \Omega + \Sigma(\Omega - \omega))^2 + \frac{1}{4} E_0^2(\ell)]}.
\end{aligned} \tag{28}$$

B. RG flow for couplings: spinless fermions

Owing to the nature of umklapp scattering which in the spinless case is different for the MC and SSH mod-

els, we shall proceed separately for each model. Thus for the MC model with a local umklapp term, the outer shell contractions $\frac{1}{2} \langle (S_{I,2}^P)^2 \rangle_{\text{o.s.}}$ and $\frac{1}{2} \langle (S_{I,2}^C)^2 \rangle_{\text{o.s.}}$ for the Peierls and Cooper channels allow us to write

$$\begin{aligned}
\partial_\ell \tilde{g}_f(\omega_1, \omega_2, \omega_3) &= \int_{-\infty}^{+\infty} \frac{d\omega}{2\pi} \left\{ \left[\tilde{g}_f(\omega_1, \omega + \omega_2 - \omega_3, \omega) \tilde{g}_f(\omega, \omega_2, \omega_3) \right. \right. \\
&\quad \left. \left. + \tilde{g}_3(\omega_1, \omega + \omega_2 - \omega_3, \omega) \tilde{g}_3(\omega, \omega_2, \omega_3) \right] I_P(\omega, \omega_2 - \omega_3) \right. \\
&\quad \left. - \tilde{g}_f(\omega_1, \omega_2, \omega + \omega_1 + \omega_2) \tilde{g}_f(\omega + \omega_1 + \omega_2, -\omega, \omega_3) I_C(\omega, \omega_1 + \omega_2) \right\},
\end{aligned} \tag{29}$$

$$\begin{aligned}
\partial_\ell \tilde{g}_3(\omega_1, \omega_2, \omega_3) &= 2 \int_{-\infty}^{+\infty} \frac{d\omega}{2\pi} \left\{ \tilde{g}_3(\omega_1, \omega, \omega_3) \tilde{g}_f(\omega + \omega_1 - \omega_3, \omega_2, \omega_1 + \omega_2 - \omega_3) I_P(\omega, \omega_1 - \omega_3) \right. \\
&\quad \left. + \tilde{g}_3(\omega, \omega_2, \omega_3) \tilde{g}_f(\omega + \omega_2 - \omega_3, \omega_1, \omega_1 + \omega_2 - \omega_3) I_P(\omega, \omega_2 - \omega_3) \right\},
\end{aligned} \tag{30}$$

which are subjected to the initial conditions (15) and (17) of the MC model.

The flow equations for the SSH model presents an important difference because of the additional k -dependent umklapp term (18). At variance with g_f and g_3 , this coupling acquires a non zero scaling dimension at the tree level. Therefore the momentum, energies and fields must be rescaled after each partial trace operation in Eq. (19), which restores the original bandwidth cutoff. Thus following the

outer shell integration, one applies the transformations $k' = sk$, $\omega' = s\omega$, $\psi^{(*)'} = s^{-1/2} \psi^{(*)}$, $T' = sT$, $L' = s^{-1}L$, and $\omega'_D = s\omega_D$ ($M'_D = s^{-2}M_D$, the spring constant κ_D is kept fixed), where $s = e^{d\ell}$. This gives the scaling transformations for the outer shell corrected couplings, namely $\tilde{g}'_{f,3}(\{\omega'\}) = s^0 \tilde{g}_{f,3}(\{\omega\})$ for the local part and $\tilde{g}'_u(\{\omega'\}) = s^{-2} \tilde{g}_u(\{\omega\})$ for the non local part. The flow equations for the SSH model then become

$$\begin{aligned}
\partial_\ell \tilde{g}_f(\omega_1, \omega_2, \omega_3) &= \int_{-\infty}^{+\infty} \frac{d\omega}{2\pi} \left\{ \left[\tilde{g}_f(\omega_1, \omega + \omega_2 - \omega_3, \omega) \tilde{g}_f(\omega, \omega_2, \omega_3) + \tilde{g}_3(\omega_1, \omega + \omega_2 - \omega_3, \omega) \tilde{g}_3(\omega, \omega_2, \omega_3) \right. \right. \\
&\quad \left. \left. + \tilde{g}_u(\omega_1, \omega + \omega_2 - \omega_3, \omega) \tilde{g}_3(\omega, \omega_2, \omega_3) + \tilde{g}_3(\omega_1, \omega + \omega_2 - \omega_3, \omega) \tilde{g}_u(\omega, \omega_2, \omega_3) \right] \right\}
\end{aligned}$$

$$\begin{aligned}
& + \tilde{g}_u(\omega_1, \omega + \omega_2 - \omega_3, \omega) \tilde{g}_u(\omega, \omega_2, \omega_3) \Big] I_P(\omega, \omega_2 - \omega_3) \\
& - \tilde{g}_f(\omega_1, \omega_2, \omega + \omega_1 + \omega_2) \tilde{g}_f(\omega + \omega_1 + \omega_2, -\omega, \omega_3) I_C(\omega, \omega_1 + \omega_2) \Big\}, \quad (31)
\end{aligned}$$

$$\begin{aligned}
\partial_\ell \tilde{g}_3(\omega_1, \omega_2, \omega_3) = 2 \int_{-\infty}^{+\infty} \frac{d\omega}{2\pi} \Big\{ & \tilde{g}_3(\omega_1, \omega, \omega_3) \tilde{g}_f(\omega + \omega_1 - \omega_3, \omega_2, \omega_1 + \omega_2 - \omega_3) I_P(\omega, \omega_1 - \omega_3) \\
& + \tilde{g}_3(\omega, \omega_2, \omega_3) \tilde{g}_f(\omega + \omega_2 - \omega_3, \omega_1, \omega_1 + \omega_2 - \omega_3) I_P(\omega, \omega_2 - \omega_3) \Big\}, \quad (32)
\end{aligned}$$

$$\begin{aligned}
\partial_\ell \tilde{g}_u(\omega_1, \omega_2, \omega_3) = & - 2 \tilde{g}_u(\omega_1, \omega_2, \omega_3) \\
& + 2 \int_{-\infty}^{+\infty} \frac{d\omega}{2\pi} \Big\{ \tilde{g}_u(\omega_1, \omega, \omega_3) \tilde{g}_f(\omega + \omega_1 - \omega_3, \omega_2, \omega_1 + \omega_2 - \omega_3) I_P(\omega, \omega_1 - \omega_3) \\
& + \tilde{g}_u(\omega, \omega_2, \omega_3) \tilde{g}_f(\omega + \omega_2 - \omega_3, \omega_1, \omega_1 + \omega_2 - \omega_3) I_P(\omega, \omega_2 - \omega_3) \Big\}, \quad (33)
\end{aligned}$$

which are subjected to the initial conditions (15), (17), and (18).

C. Response functions

Staggered $2k_F$ density-wave and zero pair momentum superconducting susceptibilities can be computed by adding a set of linear couplings to composite fields $\{h_\mu\}$ in the bare action at $\ell = 0$. This gives the source field term

$$\begin{aligned}
S_h[\psi^*, \psi] = \sum_{\omega, \Omega} \Big[& \sum_{\mu_p, M} h_{\mu_p}^M(\Omega) z_{\mu_p}^M(\omega, \omega + \Omega) \mathcal{O}_{\mu_p}^{M*}(\omega, \Omega) \\
& + \sum_{\mu_c} h_{\mu_c}(\Omega) z_{\mu_c}(-\omega, \omega + \Omega) \mathcal{O}_{\mu_c}^*(\omega, \Omega) \\
& + \text{c.c.} \Big], \quad (34)
\end{aligned}$$

where $z_{\mu_p}^M$ and z_{μ_c} are the renormalization factors of the corresponding source fields, with $z_{\mu_c(p)}^{(M)} = 1$ for the boundary conditions at $\ell = 0$. For spin- $\frac{1}{2}$ fermions, we shall focus on the $2k_F$ susceptibilities for ‘site’ $M = +$ and ‘bond’ $M = -$ charge (CDW, BOW: $\mu_p = 0$), and spin (SDW $_{x,y,z}$, BSDW $_{x,y,z}$: $\mu_{p=1,2,3}$) density-wave correlation of the Peierls channel. The corresponding composite fields are

$$\begin{aligned}
\mathcal{O}_{\mu_p}^M(\omega, \Omega) = & \frac{1}{2} [O_{\mu_p}(\omega, \Omega) + M O_{\mu_p}^*(\omega, -\Omega)], \quad (35) \\
O_{\mu_p}(\omega, \Omega) = & \sqrt{\frac{T}{L}} \sum_{k, \alpha\beta} \psi_{-, \alpha}(k - 2k_F, \omega - \Omega) \\
& \times \sigma_{\mu_p}^{\alpha\beta} \psi_{+, \beta}^*(k, \omega). \quad (36)
\end{aligned}$$

In the Cooper channel, we consider the uniform superconducting singlet (SS: $\mu_c = 0$) and triplet (TS $_{x,y,z}$: $\mu_c = 1, 2, 3$) susceptibilities. The corresponding com-

posite fields at zero pair momentum are given by

$$\mathcal{O}_{\mu_c}(\omega, \Omega) = \sqrt{\frac{T}{L}} \sum_{k, \alpha\beta} \psi_{-, \alpha}(-k, -\omega + \Omega) \sigma_{\mu_c}^{\alpha\beta} \psi_{+, \beta}(k, \omega). \quad (37)$$

For both channels, $\sigma_0 = \mathbf{1}$ and $\sigma_{1,2,3} = \sigma_{xyz}$ are the Pauli matrices.

In the case of spinless fermions, only the $2k_F$ ‘site’ CDW and BOW susceptibilities survive with

$$\begin{aligned}
\mathcal{O}_{\mu_p}^M(\omega, \Omega) = & \frac{1}{2} \sqrt{\frac{T}{L}} \sum_k [\psi_{-}(k - 2k_F, \omega - \Omega) \psi_{+}^*(k, \omega) \\
& + M \psi_{+}^*(k + 2k_F, \omega - \Omega) \psi_{-}(k, \omega)]. \quad (38)
\end{aligned}$$

In the superconducting channel, only one susceptibility is considered with the corresponding pair field

$$\mathcal{O}_{\mu_c}(\omega, \Omega) = \sqrt{\frac{T}{L}} \sum_k \psi_{-}(-k, -\omega + \Omega) \psi_{+}(k, \omega). \quad (39)$$

Adding (34) to the action S in (7), the partial integration (19) at the one-loop level yields additional outer shell contributions that correct S_h and which gives the recursion relation

$$S_h[\psi^*, \psi]_{\ell+d\ell} = S_h[\psi^*, \psi]_{\ell} + \langle \bar{S}_h \bar{S}_I \rangle_{\text{o.s.}} + \frac{1}{2} \langle \bar{S}_h^2 \rangle_{\text{o.s.}} + \dots \quad (40)$$

The second term $\langle \bar{S}_h \bar{S}_I \rangle_{\text{o.s.}}$ is proportional to $\mathcal{O}_{\mu} h_{\mu}^*$ and its complex conjugate, and leads to the flow equations for the renormalization factors z_{μ} of the pair vertex parts. In the density-wave channel, its evaluation leads to

$$\begin{aligned}
\partial_\ell z_{\mu_p}^M(\omega, \omega + \Omega) = & \int_{-\infty}^{+\infty} \frac{d\omega'}{2\pi} \Big\{ z_{\mu_p}^M(\omega', \omega' + \Omega) \\
& \times [\tilde{g}_{\mu_p}(\omega, \omega', \omega + \Omega) + M \tilde{\mathcal{G}}_3(\omega, \omega' + \Omega, \omega')] I_P(\omega', \Omega) \Big\},
\end{aligned}$$

where

$$\begin{aligned}\tilde{g}_{\mu_p=0}(\omega, \omega', \omega + \Omega) &= \tilde{g}_2(\omega', \omega, \omega + \Omega), \\ &\quad -2\tilde{g}_1(\omega, \omega', \omega + \Omega), \\ \tilde{g}_{\mu_p \neq 0}(\omega, \omega', \omega + \Omega) &= \tilde{g}_2(\omega', \omega, \omega + \Omega), \\ \tilde{G}_3(\omega, \omega' + \Omega, \omega') &= \tilde{g}_3(\omega, \omega' + \Omega, \omega') \\ &\quad -2\tilde{g}_3(\omega, \omega' + \Omega, \omega + \Omega),\end{aligned}\quad (42)$$

for fermions with spins, and

$$\begin{aligned}\tilde{g}_{\mu_p}(\omega, \omega', \omega + \Omega) &= \tilde{g}_f(\omega, \omega', \omega + \Omega), \\ \tilde{G}_3(\omega, \omega' + \Omega, \omega') &= -\tilde{g}_3(\omega, \omega' + \Omega, \omega'),\end{aligned}\quad (43)$$

in the spinless case. Similarly, for the superconducting channel, one gets

$$\begin{aligned}\partial_\ell z_{\mu_c}(\omega, -\omega + \Omega) &= \int_{-\infty}^{+\infty} \frac{d\omega'}{2\pi} \left\{ z_{\mu_c}(\omega', -\omega' + \Omega) \right. \\ &\quad \times \tilde{g}_{\mu_c}(\omega, \omega', \Omega) I_C(\omega', \Omega) \Big\},\end{aligned}\quad (44)$$

where

$$\begin{aligned}\tilde{g}_{\mu_c=0}(\omega, \omega', \Omega) &= -\tilde{g}_1(\Omega - \omega, \omega, \omega') - \tilde{g}_2(\omega, \Omega - \omega, \omega'), \\ \tilde{g}_{\mu_c \neq 0}(\omega, \omega', \Omega) &= \tilde{g}_1(\Omega - \omega, \omega, \omega') - \tilde{g}_2(\omega, \Omega - \omega, \omega').\end{aligned}\quad (45)$$

for spin- $\frac{1}{2}$ fermions, and

$$\tilde{g}_{\mu_c}(\omega, \omega', \Omega) = -\tilde{g}_f(\omega, \Omega - \omega, \omega') \quad (46)$$

in the spinless case.

As a result of the partial trace integration, the last term of (40), which is proportional to $h_{\mu_c(p)}^{(M)*} h_{\mu_c(p)}^{(M)}$, is generated along the flow and corresponds to the susceptibility in each channel considered, namely

$$\begin{aligned}\partial_\ell \chi_{\mu_c(p)}^{(M)}(\Omega) &= (\pi v_F)^{-1} \int_{-\infty}^{+\infty} \frac{d\omega}{2\pi} \left\{ |z_{\mu_c(p)}^{(M)}(\mp\omega, \omega + \Omega)|^2 \right. \\ &\quad \times (2s + 1) I_{C(P)}(\omega, \Omega) \Big\},\end{aligned}\quad (47)$$

which has been defined positive ($\chi_{\mu_c(p)}^{(M)}(\Omega) = 0$ at $\ell = 0$), and where s is the spin.

We close this section by a digression on the numerical aspects associated with the solution of the above equations. Their numerical evaluation makes use of patches in the frequency manifold. The frequency axis is discretized into a total of 15 subdivisions or patches between the maximum values $\omega_{\max} = \pm 1.5 E_F$, which serve as bounds of integration for the frequency. The interaction is taken as constant over each patch where the loop integrals are done exactly. In order to reduce the number of frequency dependent coupling constants, we take

(41) advantage of certain symmetries namely, the time inversion, left-right Fermi points symmetry, and the exchange symmetry between the incoming (ω_1, ω_2) and outgoing $(\omega_3, \omega_4 = \omega_1 + \omega_2 - \omega_3)$ frequencies. The last symmetry antisymmetrizes the initial conditions for the spinless fermions case, especially for the umklapp process \tilde{g}_3 . We thus have to calculate 932 different functions for each \tilde{g}_i . The same procedure is used to calculate the response functions and susceptibilities. The flow equations are numerically solved until the most singular susceptibility diverges with the slope $\pi v_F \partial_\ell \chi_\mu^M = 10^6$, which determines the critical value ℓ_c at which the algorithm is stopped.

IV. RESULTS

A. Adiabatic limit

The results at non zero-phonon frequency will be compared to those of the adiabatic limit where $\omega_{0(D)} \rightarrow 0$. In this limit, the initial conditions given in Sec. II for both models show that either $\omega_{3-1} \rightarrow 0$ or $\omega_{3-2} \rightarrow 0$, indicating that no phonon exchange between fermions at finite frequency is possible. In the spinless case the g_f coupling Eq. (15) reduces to its backward scattering part. Therefore only close loops contribute to the renormalization of both the coupling constants, susceptibilities, and one-particle self-energy Σ ; the latter being vanishingly small in the adiabatic limit.

The flow equations for fermions with $s = 1/2$ (resp. $s = 0$) (24-26) [resp. Eqs. (29-30)] can be recast into equations for g_1 and g_3 , which become independent of frequencies

$$\partial_\ell (\tilde{g}_1 \pm \tilde{g}_3) = -(2s + 1)(\tilde{g}_1 \pm \tilde{g}_3)^2/2. \quad (48)$$

The solution is obtained at once

$$\tilde{g}_1(\ell) \pm \tilde{g}_3(\ell) = \frac{\tilde{g}_1 \pm \tilde{g}_3}{1 + \frac{1}{2}(2s + 1)(\tilde{g}_1 \pm \tilde{g}_3)\ell}, \quad (49)$$

which presents a singularity at $\ell_0 = -2[(2s + 1)(\tilde{g}_1 \pm \tilde{g}_3)]^{-1}$ for combinations of bare attractive couplings $\tilde{g}_1 \pm \tilde{g}_3$ found in the MC (+) and SSH (-) models (Eqs. (13)-14), and (15-16)). This signals an instability of the fermion system and the formation of a Peierls state with a - mean-field (MF) - gap $\Delta_0 (\equiv 2E_F e^{-\ell_0})$, which takes the BCS form¹⁵

$$\Delta_0 = 2E_F \exp \left(-2/(2s + 1)|\tilde{g}_1 \pm \tilde{g}_3| \right). \quad (50)$$

This singularity is present in the pair vertex factors $z_{\mu_p=0}^M$ at $\Omega = 0$ in either CDW or BOW channel depending of the model. In the adiabatic limit this can be seen by retaining only closed loops in (41), where for frequency independent couplings, $z_{\mu_p=0}^M$ becomes in turn independent of ω and obeys the following flow equation at $\Omega = 0$

$$\partial_\ell \ln z_{\mu_p=0}^M = -(2s + 1)(\tilde{g}_1 + M\tilde{g}_3)/2. \quad (51)$$

With the help of Eq. (49), this is readily solved to lead the simple pole expression $z_{\mu_p=0}^M = [1 + \frac{1}{2}(2s+1)(\tilde{g}_1 + M\tilde{g}_3)\ell]^{-1}$. From (47), the $2k_F$ susceptibility takes the form

$$\pi\nu_F\chi_{\mu_p=0}^M(\ell) = \frac{\ell}{1 + \frac{1}{2}(2s+1)(\tilde{g}_1 + M\tilde{g}_3)\ell}. \quad (52)$$

The expected simple pole divergence at ℓ_0 then occurs in the site CDW ($M = +$) response for the MC model and in the BOW ($M = -$) response for the SSH model. No enhancement is found for the susceptibilities in the superconducting channel.

Strictly speaking, the above adiabatic MF results hold for models where only momentum independent couplings are retained. In the case of the SSH model for spinless fermions, however, the adiabatic limit of Eqs. (31-33) does not coincide with the MF result due to the presence of g_u . In the adiabatic limit the flow equations read

$$\begin{aligned} \partial_\ell \tilde{g}_1 &= -\frac{1}{2}\tilde{g}_1^2 - \frac{1}{2}(\tilde{g}_u + \tilde{g}_3)^2, \\ \partial_\ell \tilde{g}_3 &= -\tilde{g}_3\tilde{g}_1, \\ \tilde{g}_u(\ell) &= \tilde{g}_u \exp \left[-2 \int_0^\ell (1 + \tilde{g}_1(\ell')) d\ell' \right]. \end{aligned} \quad (53)$$

The solution of these equations shows that the value of the adiabatic SSH gap Δ_0 for spinless fermions is slightly reduced compared to the MF prediction (50) where g_u is absent.

B. The molecular crystal model

1. Spinless case

The solution of the flow equations (29-30) for the MC model in the spinless case ($s = 0$) is obtained by using the antisymmetrized boundary conditions given in (15-16) at $\ell = 0$. The typical flow of susceptibilities in the Peierls and Cooper channels at an intermediate phonon frequency is shown in Figure 1. Like for the MF result (52), the singularity is found to occur solely in the site ($M = +$) CDW susceptibility at ℓ_c . There is no noticeable enhancement of other responses including those of the superconducting channel. The singularity signals the existence of a Peierls gap Δ ($\equiv 2E_F e^{-\ell_c}$) with an amplitude that is reduced at non zero ω_0 compared to its adiabatic value Δ_0 (Eq. (50)). Figure 2 shows this renormalization as a function of the ratio ω_0/Δ_0 of the phonon frequency to the MF gap (here the molecular mass M_0 is varied while the spring constant κ_0 is kept fixed). For small ω_0/Δ_0 the gap is weakly renormalized and remains close to its classical value. However, when the ratio ω_0/Δ_0 approaches unity, the gap undergoes a rapid decrease due to quantum fluctuations. This results from the growing of vertex corrections and interference between Peierls and Cooper scattering channels.

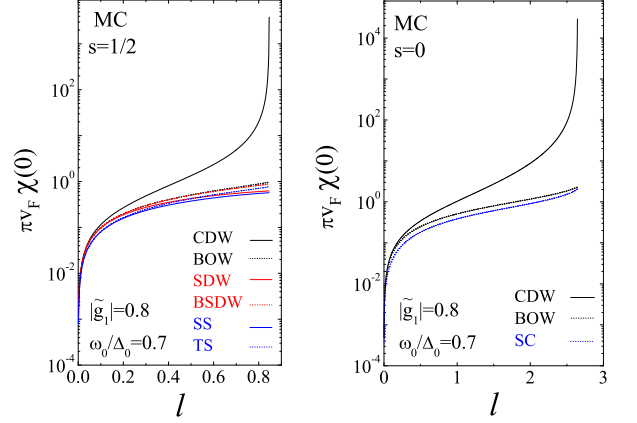


FIG. 1: Typical variation of the susceptibilities with the scaling parameter ℓ for the MC model for spinless fermions ($s = 0$, right) and spin- $\frac{1}{2}$ fermions ($s = 1/2$, left). The locus of the singularity at ℓ_c gives the value of the gap $\Delta = E_0(\ell_c)$.

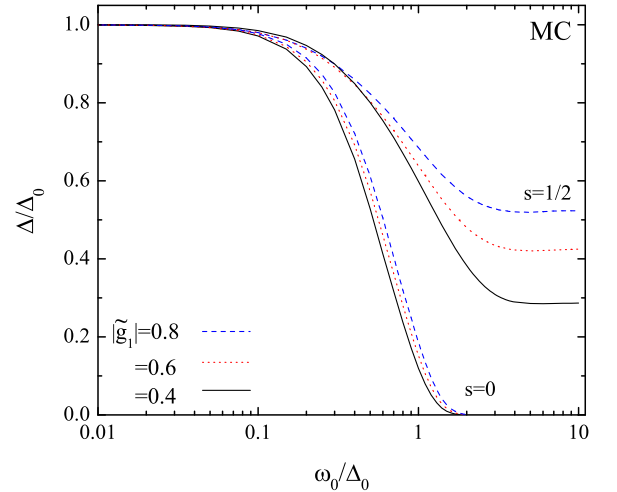


FIG. 2: The site CDW gap of the MC model for spinless ($s = 0$) and spin- $\frac{1}{2}$ ($s = 1/2$) fermions as a function of the phonon frequency and for different couplings. Both quantities are normalized to the MF gap.

These fluctuations signal a change of regime (defined at the point of a change of curvature for the gap profile) that we refer to as a quantum-classical crossover for the gap.

The remaining gap tail terminates with a transition to a $\Delta = 0$ disordered state at a threshold frequency slightly above Δ_0 . The ratio ω_0/Δ_0 at which the transition occurs is weakly dependent on the initial \tilde{g}_i for the range of coupling covered by the present RG. This result corroborates the old two cut-off scaling arguments for

the disappearance of an ordered state at $\omega_0 \sim \Delta_0$,¹⁵ and agrees with the DMRG,⁹ and Monte Carlo⁵ results for the MC model. The nature of the transition to the quantum gapless state is also of interest. We follow the notation of Ref.⁸ and define the coupling $\alpha \equiv \frac{1}{2}\sqrt{|\tilde{g}_1|\omega_0 E_F}$. We see from Figure 3 that the variation of the gap Δ , close to the critical α_c at which the transition occurs, follows closely the Baxter formula for a Kosterlitz-Thouless (KT) transition³⁷

$$\Delta \propto \frac{2E_F}{\sqrt{\alpha^2 - \alpha_c^2}} e^{-b/\sqrt{\alpha^2 - \alpha_c^2}}, \quad (54)$$

where b is positive a constant. This behaviour found in the weak coupling range is similar to the one obtained by the DMRG method and perturbative expansion in strong coupling.^{5,9}

For phonon frequency above the threshold, the new state is expected to be a Luttinger liquid.^{9,15} This is seen at the one-loop RG level from the existence of a power law behaviour of the site CDW susceptibility, namely $\chi_{\mu p=0}^+(\ell) \sim [E_0(\ell)]^{-\gamma}$. The latter takes place only above some characteristic ℓ^* (Fig. 4) that depends on ω_0 and which decreases with the strength of the coupling. Non universality is also found for the Luttinger liquid exponent γ for $E_0(\ell) \ll E_0(\ell^*)$. Following the one-dimensional theory,^{38,39} the exponent can be written as $\gamma = 2 - 2K_\rho$, where K_ρ is the stiffness parameter for the density degrees of freedom that enters in the bosonization scheme. Within the limitation of a weak coupling theory, it is therefore possible to determine the dependence of K_ρ on interaction and phonon frequency. As shown in Figure 5, the one-loop RG results confirms the non universal character of the stiffness parameter. Going down on the frequency scale, K_ρ is sizeably reduced at the approach of the KT transition where retardation effects have a strong influence on the properties of the Luttinger liquid parameter. We find that K_ρ stays above the minimum value of $\frac{1}{2}$ known for isotropic spin chain in the gapless domain^{39,42} – following the Wigner-Jordan transformation of spins into spinless fermions. On the other hand, K_ρ is only weakly dependent on the couplings at large ω_0 , where it tends to the non adiabatic – coupling independent – value $K_\rho = 1$ at $\omega_0 \rightarrow \infty$. Recall that the initial couplings of the MC model (Eqs. (15) and (17)) vanish in this limit, and the system is equivalent to a non interacting Fermi gas.

From the variation of the critical coupling α_c with the phonon frequency ω_0 , one can construct the phase diagram of Fig. 6. The phase boundary between the insulating and the metallic Luttinger liquid states is found to follow closely a power law dependence of the form $\alpha_c \sim \omega_0^\eta$, with the exponent $\eta \approx 0.7$. This feature captured by a one-loop calculation is analogous to the quantum-classical boundary of the phase diagram of the 1D XY spin-Peierls model determined by the DMRG method.⁸ The latter model is also characterized by a zero temperature KT transition as we will see for the spinless SSH model in Sec. IV C.

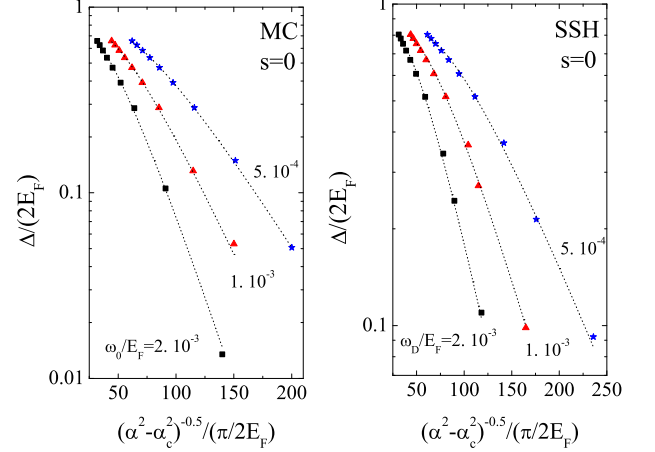


FIG. 3: The site CDW (left) and BOW (right) gaps as a function of the critical parameter of the KT transition to a Luttinger liquid for the CM and SSH models in the spinless case. The dotted line is a least squares fit to the Baxter formula Eq. (54).

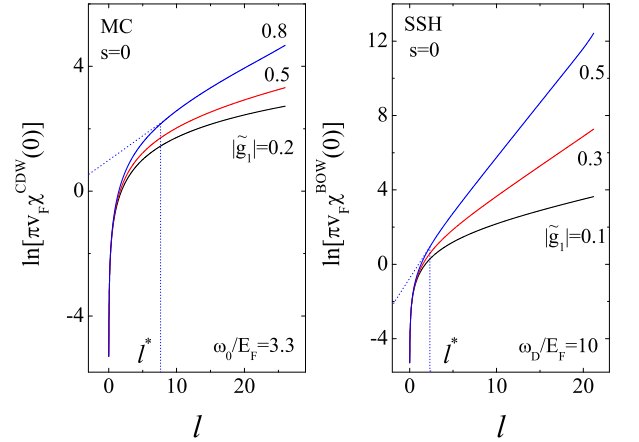


FIG. 4: Typical power law divergence of the site CDW (left) and BOW (right) susceptibilities at $\ell \gg \ell^*$ in the gapless Luttinger liquid regime.

2. Spin- $\frac{1}{2}$ fermions

The results for the MC model with spin- $\frac{1}{2}$ fermions ($s = 1/2$) ensue from the solution of Eqs. (24-26) and the computation of the susceptibilities (47), from (41-42) and (44-45). Like spinless fermions, the singularity is found in the $M = +$, site CDW susceptibility at finite ℓ_c (Fig. 1). The corresponding value for the gap Δ is reduced with respect to the adiabatic mean-field result Δ_0 in (50). The onset of quantum fluctuations due to growing interference between different scattering channels is again responsible

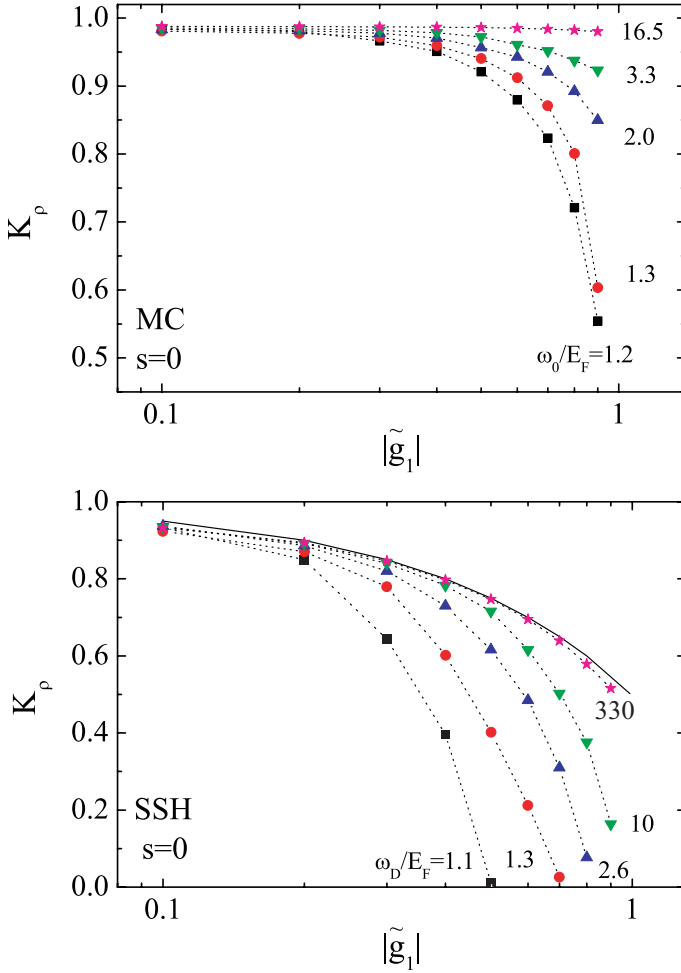


FIG. 5: One-loop calculation of the density stiffness parameter K_ρ of the MC (upper panel) and SSH (lower panel) models in the spinless case as a function of the initial coupling $|\tilde{g}_1|$, and for different phonon frequencies. The continuous line in the lower panel corresponds to the antiadiabatic one-loop result $K_\rho = 1 - \frac{1}{2}|\tilde{g}_1|$.

for a quantum-classical crossover when ω_0 approaches Δ_0 where there is change of curvature in the gap profile, but the gap never goes to zero. It remains finite at large phonon frequencies and is dependent on the bare attractive amplitude \tilde{g}_i . At large frequency the singularity at ℓ_c occurs essentially independently for spin $[\tilde{g}_1(\{\omega\})]$ and charge $[2\tilde{g}_2(\{\omega\}) - \tilde{g}_1(\{\omega\}), \tilde{g}_3(\{\omega\})]$ combinations of couplings at zero Peierls and Copper frequency. As a function of ω_0 , the system then undergoes a crossover from a renormalized classical Peierls state towards a quantum but still site-CDW ordered state in which both spin and charge degrees of freedom are gapped due to attractive couplings and the relevance of umklapp processes at arbitrary large but finite ω_0 . An ordered state is well known to be found at large ω_0 in Monte carlo simulations.⁵ This quantum-classical crossover marks the onset of a decoupling between spin and charge degrees of freedom, a separation found in the Luther-Emery model.^{23,38,40}

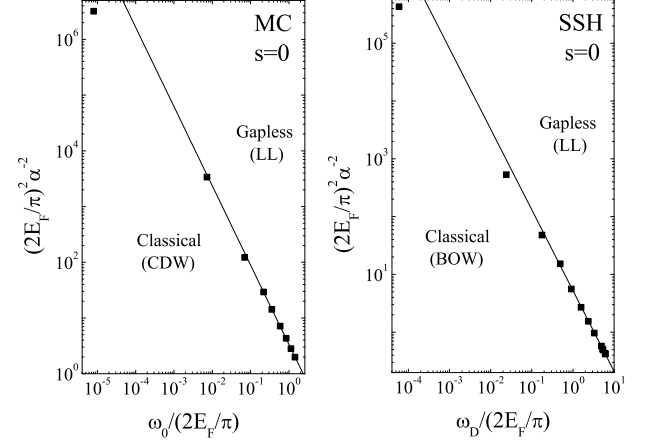


FIG. 6: Phase diagram of MC (left) and SSH (right) models for spinless fermions. The full squares are the RG results and the continuous lines is the power law $\alpha_c^2 \sim \omega_0^{1.4}$ of the critical coupling of the KT transition on the phonon frequency.

It is worth noting that in the purely non adiabatic case where ω_0 is strictly infinite, the initial couplings (13) are independent of frequency and satisfy the conditions $\tilde{g}_1 < 0$, and $\tilde{g}_1 - 2\tilde{g}_2 = |\tilde{g}_3|$, which coincide with those of an attractive Hubbard model. Its exact solution is well known to give a disordered ground state. At the one-loop level, the RG equations (24-26) at zero external frequencies show indeed that \tilde{g}_1 alone is singular, with a gap in the spin sector only. Umklapp processes are irrelevant and charge degrees of freedom remain gapless, consistently with the absence of long-range order at $\omega_0 = \infty$.^{23,24,25,41} Working at arbitrarily large but finite ω_0 introduces finite retardation effect that is sufficient to make initial conditions deviate from those of the attractive Hubbard model. This restores the relevance of umklapp term in the charge sector and in turn long-range order.⁵

C. SSH

1. Spinless case

We turn now to the study of the SSH model. In the spinless case the presence of the non local umklapp term g_u introduces some qualitative differences with the MC model for which this term is absent. Thus the solution of (31-33), and (41,44,47) in the spinless case shows that for small ω_D/Δ_0 , the BOW susceptibility ($\mu_{p=0}, M = -$) is the only singular response that leads to a gap at zero temperature (Fig. 7).

As one moves along the ω_D/Δ_0 axis (along which the mass M_D varies and κ_D is constant), one finds again from Fig. 8, that for $\omega_D/\Delta_0 < 0.1$, the gap is weakly renor-

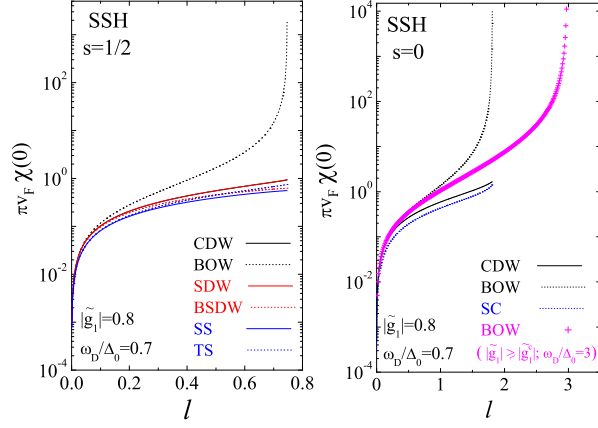


FIG. 7: Typical variation of the susceptibilities for the SSH model as a function of the scaling parameter ℓ for spinless fermions ($s = 0$, right) and spin- $\frac{1}{2}$ fermions with spins ($s = 1/2$, left).

malized compared to its adiabatic classical value computed from (53). As the ratio increases further, there is a strong downward renormalization for the gap which undergoes a quantum-classical crossover. However, at variance with the MC model, the ratio ω_D/Δ_0 at which there is a change of curvature in the variation of the gap shows a stronger dependence on the amplitude of the initial coupling – parametrized by the backward scattering part $|\tilde{g}_1|$ of \tilde{g}_f in (15) (triangles, inset of Fig. 8).

At higher phonon frequency we come up against a critical value where the gap completely vanishes and the system enters in a metallic state at zero temperature. This critical ratio is also coupling dependent (squares, inset of Fig. 8). In the non adiabatic limit when $(\omega_D/\Delta_0)^{-1} \rightarrow 0$, the critical coupling heads on to the one-loop limiting value $|\tilde{g}_1^c| = 1$, which can be extracted directly from Eq. (33) in this limit. A frequency dependent threshold $|\tilde{g}_1^c|$ for the existence of an ordered state is a direct consequence of the relevance of the non local umklapp term \tilde{g}_u in (33), which differs markedly from the MC model and simple two-cutoff scaling arguments especially at large phonon frequency. The phase diagram shown in the inset of Fig. 8 can then be obtained for the spinless SSH model. A critical line for $(\omega_D/\Delta_0)^{-1}$ vs $|\tilde{g}_1^c|$ can be drawn, separating the quantum disordered state from BOW order. The singularity of the BOW susceptibility in the quantum domain is shown in Fig. 7.

The numerical solution of the flow equations is not carried out easily in the limit of very small couplings owing to the large number of frequencies needed to reach the desired accuracy. Our results, obtained down to $|\tilde{g}_1| = 0.1$, tend to show, however, that the critical line $|\tilde{g}_1^c|$ extrapolates to zero at the finite value of the ratio $\Delta_0/\omega_D \approx 1.1$, which joins the value obtained from the two-cutoff scaling arguments.¹⁵ Above this value, an ordered BOW state

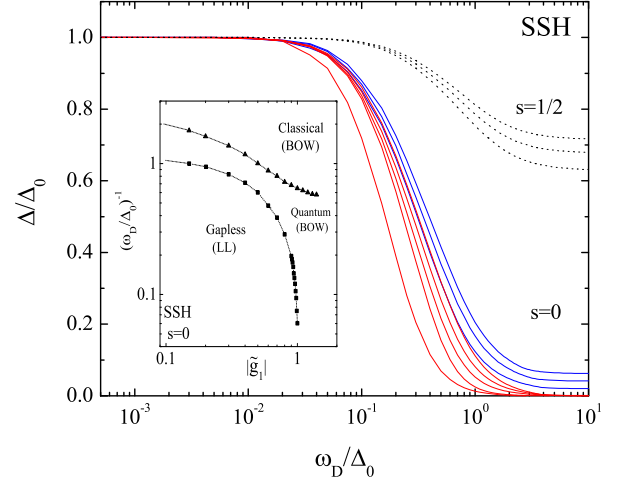


FIG. 8: The BOW gap normalized to its adiabatic value as a function the ratio of the phonon frequency and the adiabatic gap for the SSH model for spinless fermions (continuous lines, left to right, red: $|\tilde{g}_1| = 0.1, 0.4, 0.6, 0.9 < |\tilde{g}_1^c|$; blue: $|\tilde{g}_1| = 1.1, 1.15, 1.2 > |\tilde{g}_1^c|$) and spin- $\frac{1}{2}$ fermions (dotted lines; from bottom to the top: $|\tilde{g}_1| = 0.5, 0.7, 0.8$). Inset: phase diagram of the spinless SSH model. Quantum BOW order/gapless Luttinger liquid (LL) (squares), and the quantum-classical crossover for the BOW order state (triangles).

would then be found at any finite coupling. When the ratio finally crosses the quantum-classical line, the system enters in a Peierls BOW state similar to the one of the classical adiabatic limit. This quantum-classical boundary, clearly identified in Fig. 8 as a change of regime for the gap, is consistent with the one found by DMRG for the XY spin-Peierls chain (following the conversion of spins into spinless Wigner-Jordan fermions).⁸

As one moves from the quantum massive domain towards the critical line at higher frequency, the gap collapses to zero. Following the example of what has been done for the MC model, we follow the notation of Ref.⁸ and define $\alpha_c \equiv \frac{1}{2} \sqrt{|\tilde{g}_1^c| \omega_D E_F}$, as the critical coupling where the gap vanishes. We thus find that close to the transition, Δ decreases to zero according to the Baxter expression Eq. (54) for a KT transition (Fig. 3). This result which carries over the whole critical line at finite frequency is in accord with DMRG results obtained on the spin-Peierls XY⁸ and XXZ¹⁰ chains. For the latter model a KT transition was also found by Citro *et al.*,¹⁸ using the RG method in the bosonization framework. In the same vein, Kuboki and Fukuyama also show by perturbation theory that retardation is equivalent at large frequency to frustration in the spin interactions,¹⁶ which beyond some threshold is well known to promote a KT transition to a dimerized state.⁴²

As shown by the phase diagram of Fig. 6, the critical coupling is found to follow the power law variation

$\alpha_c \sim \omega_D^\eta$, with $\eta \approx 0.7$, over a sizeable range of the phonon frequency (deviations are found in the limit of small frequency). Such a power law agrees with the one found in DMRG for the XY spin-Peierls chain,⁸ and is similar to the one obtained in the MC case for spinless fermions.

As regards to the nature of the gapless liquid state in the disordered region, the situation is qualitatively similar to the MC model. We find the presence of a non universal power law divergence for the BOW response function $\chi_{\mu_p=0}^-(2k_F) \propto [E_0(\ell)]^{-\gamma}$ below some characteristic energy scale $E_0(\ell^*)$ (Fig. 4), which indicates the presence of a Luttinger liquid. The weak coupling determination of the charge stiffness parameter $K_\rho(\gamma = 2 - 2K_\rho)$ ³⁸ at the one-loop level is shown in Figure 5. By comparison with the MC model, K_ρ is smaller and shows a stronger variation with the strength of the coupling even for large phonon frequencies. This is so for in the non adiabatic limit, the initial conditions for both $\tilde{g}_f(\{\omega\})$ and $\tilde{g}_u(\{\omega\})$ are non zero and a massive phase remains possible. In this limit, the RG results join the one-loop relation $K_\rho = 1 - \frac{1}{2}|\tilde{g}_1|$ (continuous line, lower panel of Fig. 5), which is known to be a good approximation to the exact result.^{37,43} It is worth noticing that although the transition remains of infinite order for any path that crosses the critical line from the massive sector to the Luttinger liquid one, the characteristics of the latter phase, through its exponent γ (or its stiffness coefficient K_ρ) is strongly dependent on retardation effect. With the caveat of the limited accuracy of one-loop calculations for sizeable γ , the present results would indicate that except for the domain of large frequency, K_ρ penetrates deeply into the ‘Ising sector’ where $K_\rho < 1/2$ at the approach of the critical line.

A similar downward renormalization of K_ρ by retardation effects has also been found by Citro *et al.*,¹⁸ using the self-consistent harmonic approximation and the RG method in the bosonization frame for the XXZ spin model of the spin Peierls instability. When the spins are converted into fermions through a Wigner-Jordan transformation, the properties of this model are encompassed by the flow equations (31-33) following a redefinition of the initial conditions (15-18).

2. Spin- $\frac{1}{2}$ fermions

The results for the SSH model with spin- $\frac{1}{2}$ fermions is obtained from the solution of Eqs. (24-26) using the initial conditions (14). The computation of the susceptibilities (47) using (41-42) and (44-45) shows that the singularity and the formation of the gap remains as expected in the BOW channel (Fig. 7). As a result of growing interference between the Peierls and Cooper channels and vertex corrections in the scattering amplitudes, the reduction of the BOW classical gap as a function of the frequency, (Fig. 8) is less pronounced than for the MC model. This reduction then evolves to a quantum-

classical crossover at $\omega_0 \sim \Delta_0$. Following the example of the MC model, the system remains massive for both spin and charge and is thus BOW ordered in the quantum regime. The amplitude of the gap at large frequency is however bigger. As a matter of fact, in the non adiabatic case where ω_D is infinite, the initial couplings (14) are frequency independent but at variance with the MC model, they satisfy the inequalities $\tilde{g}_1 < 0$, $\tilde{g}_1 < \tilde{g}_3$. These are compatible with the Luther-Emery conditions for a mass in both spin and charge sectors.^{23,40,44}

V. CONCLUSION

In this work we used an extension of the RG approach to one-dimensional fermion gas that includes the full influence of retardation in the interactions induced by phonons. Within the inherent bounds of a weak coupling theory, the method has been put to the test and proved to be rather satisfying, providing a continuous description of the gap as a function of the phonon frequency for electron-phonon models with either spinless or spin- $\frac{1}{2}$ fermions. Generally speaking, the results brought out the importance of the static scale Δ_0 of the adiabatic theory for the occurrence of a quantum-classical crossover for the gap as one cranks up the phonon frequency, confirming in passing the old arguments of the two-cutoff scaling approach. The RG calculations allowed us to study the nature of the transition to the gapless liquid phase for spinless fermions. For both the MC and SSH models, this transition was found to be of infinite order, consistently with existing numerical results.

The RG method for the SSH model required to take into account the momentum dependent umklapp term. The latter is responsible for the continuation of the infinite order critical line to arbitrary large phonon frequency where it connects to the well known results of frustrated spin chains. The existence in the gapless phase of a sharp power law behaviour of $2k_F$ density response at low energy showed that this phase can be identified with a Luttinger liquid. The non universal variation of the power law exponent with the strength of interaction and retardation was obtained at the one-loop level. Retardation effects induce a downward renormalization of the Luttinger parameter K_ρ for both models in the disordered phase. However, this renormalization is apparently much stronger in the SSH case where K_ρ goes under its limiting $\frac{1}{2}$ value known for the anisotropic spin chain in the gapless regime.

While this work did not dwell on the combined influence of direct and retarded interactions on Peierls-type instabilities, Coulomb interaction can be actually incorporated without difficulty following a mere change of the boundary conditions for the RG flow of scattering amplitudes. A further extension of the method that includes both the frequency and momentum functional dependence of the scattering amplitudes would be also worth while. As was shown very recently by Tam *et al.*,³³ in the

context of the one-dimensional MC-Hubbard model and by Honerkamp *et al.*,³³ in the two-dimensional situation, the difficulties inherent to such an extension proved not insurmountable. An RG implementation of this sort for interacting quasi-one-dimensional electron systems would be quite desirable. It would yield a more complete description of electronic phases found in correlated materials like the organic conductors and superconductors. The coupling of electrons to both intramolecular and intermolecular (acoustic) phonon modes are in practice both present in these systems and their characteristic energies are often close to the energy scales associated to the various types of long-range order observed.⁴⁵ These systems then fall in the intermediate phonon frequency range considered in this work, and for which retardation effects

may play a role in the structure of their phase diagram. The impact of retarded interactions on electronic states found in quasi-one-dimensional conductors is currently under investigation.

Acknowledgments

We thank L. G. Caron and K.-M. Tam for useful discussions and comments. H. B. thanks I. A. Bindloss for an helpful correspondence. C. B. also thanks the Natural Sciences and Engineering Research Council of Canada (NSERC), and the Canadian Institute for Advanced Research (CIFAR) for financial support.

-
- ¹ M. Braden, G. Wilkendorf, J. Lorenzana, M. Ain, G. J. McIntyre, M. Behruzi, and G. Heger, Phys. Rev. B **54**, 1105 (1996).
 - ² J. P. Pouget, Eur. Phys. J B **20**, 321 (2001).
 - ³ D. Chow, P. Wzietek, D. Foglatti, B. Alavi, D. J. Tantillo, C. A. Merlic, and S. E. Brown, Phys. Rev. Lett. **81**, 3984 (1998).
 - ⁴ E. Fradkin and J. E. Hirsch, Phys. Rev. B **27**, 1680 (1983).
 - ⁵ J. E. Hirsch and E. Fradkin, Phys. Rev. B **27**, 4302 (1983).
 - ⁶ W. P. Su, J. R. Schrieffer, and A. J. Heeger, Phys. Rev. Lett. **42**, 1698 (1979), see also S. Barisic, Phys. Rev. B **5**, 932 (1972).
 - ⁷ T. Holstein, Ann. Phys. **8**, 325 (1959).
 - ⁸ L. G. Caron and S. Moukouri, Phys. Rev. Lett **76**, 4050 (1996).
 - ⁹ R. J. Bursill, R. H. McKenzie, and C. J. Hamer, Phys. Rev. Lett. **80**, 5607 (1998).
 - ¹⁰ R. J. Bursill, R. H. McKenzie, and C. J. Hamer, Phys. Rev. Lett. **83**, 408 (1999).
 - ¹¹ D. Augier, D. Poilblanc, E. Sorensen, and I. Affleck, Phys. Rev. B **58**, 9110 (1998); A. Weisse and H. Fehske, Phys. Rev. B **58**, 13526 (1998); G. Wellein and H. Fehske, and A. P. Kampf, Phys. Rev. Lett. **81**, 3956 (1998).
 - ¹² C. E. Creffield, G. Sangiovanni, and M. Capone, Eur. Phys. J. B **44**, 175 (2005); P. Sengupta, A. W. Sandvik, and D. K. Campbell, Phys. Rev. B **67**, 245103 (2003); R. H. McKenzie, C. J. Hamer, and D. W. Murray, Phys. Rev. B **53**, 9676 (1996).
 - ¹³ M. Nakahara and K. Maki, Phys. Rev. B **25**, 7789 (1982); D. K. Campbell and A. R. Bishop, *Ibid.*, **24**, 4859 (1981).
 - ¹⁴ G. S. Grest, E. Abrahams, S.-T. Chui, P. A. Lee, and A. Zawadowski, Phys. Rev. B **14**, 1225 (1976).
 - ¹⁵ L. G. Caron and C. Bourbonnais, Phys. Rev. B **29**, 4230 (1984).
 - ¹⁶ K. Kuboki and H. Fukuyama, J. Phys. Soc. Jpn. **56**, 3126 (1987).
 - ¹⁷ G. S. Uhrig, Phys. Rev. B **57**, R14004 (1998).
 - ¹⁸ R. Citro, E. Orignac, and T. Giamarchi, Phys. Rev. B **72**, 024434 (2005).
 - ¹⁹ R. H. McKenzie and J. W. Wilkins, Phys. Rev. Lett. **69**, 1085 (1992); Q. Wang, H. Zheng, and M. Avignon, Phys. Rev. B **63**, 115114 (2001); H. Zheng, D. Feinberg, and M. Avignon, Phys. Rev. B **39**, 9405 (1989); S. Blawid and A. J. Millis, Phys. Rev. B **63**, 014305 (2000); S. Datta and S. Yarlagadda, Phys. Rev. B **75**, 035124 (2007).
 - ²⁰ D. Schmeltzer, R. Zeyher, and W. Hanke, Phys. Rev. B **33**, 5141 (1986); C. Bourbonnais and L. G. Caron, J. Phys. (France) **50** 2751 (1989); D. Schmeltzer and A. R. Bishop, Phys. Rev. B **59**, 4541 (1999); P. Sun, D. Schmeltzer, and A. R. Bishop, Phys. Rev. **62**, 11308 (2000); C. Q. Wu, Q. F. Wang, and X. Sun, Phys. Rev. B **52**, 7802 (1995).
 - ²¹ J. Voit and H. J. Schulz, Phys. Rev. B **34**, 7429 (1986); **36**, 968 (1987).
 - ²² G. T. Zmnyani, S. A. Kivelson, and A. Luther, Phys. Rev. Lett. **60**, 2089 (1988). I. A. Bindloss, Phys. Rev. B **71**, 205113 (2005).
 - ²³ V. J. Emery, in *Highly Conducting One-Dimensional Solids*, edited by J. T. Devreese, R. E. Evrard, and V. E. van Doren (Plenum Press, New York, 1979), p. 247.
 - ²⁴ J. Solyom, Adv. Phys. **28**, 201 (1979).
 - ²⁵ M. Kimura, Prog. Theor. Phys. **63**, 955 (1975).
 - ²⁶ C. Bourbonnais and L. G. Caron, Int. J. Mod. Phys. B **5**, 1033 (1991).
 - ²⁷ D. Zanchi and H. J. Schulz, Phys. Rev. B **61**, 13 609 (2000).
 - ²⁸ C. Honerkamp, M. Salmhofer, N. Furukawa, and T. M. Rice, Phys. Rev. B **63**, 35109 (2000).
 - ²⁹ C. J. Halborth and W. Metzner, Phys. Rev. B **85**, 5164 (2000).
 - ³⁰ R. Duprat and C. Bourbonnais, Eur. Phys. J. B **21**, 219 (2001).
 - ³¹ J. C. Nickel, R. Duprat, C. Bourbonnais, and N. Dupuis, Phys. Rev. B **73**, 094616 (2006).
 - ³² M. Tsuchiizu, Phys. Rev. B **74**, 155109 (2006).
 - ³³ During the completion of this work, we became aware of extensions of the RG method to frequency dependent interactions similar to the one developed in the present work. On one-dimensional and ladder systems, see *e.g.*, K.-M. Tam, S.-W. Tsai, D. K. Campbell, and A. H. Castro Neto, Phys. Rev. B **75**, 161103 (2007); *Ibid.*, Phys. Rev. B **75**, 195119 (2007) ; on two-dimensional Hubbard model, see C. Honerkamp, H. C. Fu, and D.-H. Lee, Phys. Rev. B **75**, 014503 (2007); *Ibid.*, arXiv:cond-mat/05090702; on superconductivity in strong coupling, see S.-W. Tsai, A. H. Castro Neto, R. Shankar and D. K. Campbell, Phys. Rev. B **72**, 054531 (2005).
 - ³⁴ C. Bourbonnais, B. Guay, and R. Wortis, in *Theoretical*

- methods for strongly correlated electrons*, edited by A. M. Tremblay, D. Sénéchal, and C. Bourbonnais (Springer, Heidelberg, 2003), p. 77, cond-mat/0204163.
- ³⁵ M. P. M. den Nijs, Phys. Rev. B. **23**, 6111 (1981).
- ³⁶ J. L. Black and V. J. Emery, Phys. Rev. B. **23**, 429 (1981).
- ³⁷ R. J. Baxter, *Exactly Solved Models in Statistical Mechanics* (Academic Press, London, 1982).
- ³⁸ T. Giamarchi, *Quantum Physics in One Dimension* (Oxford University Press, Oxford, 2004).
- ³⁹ R. Shankar, Int. J. Mod. Phys. B **4**, 2371 (1990).
- ⁴⁰ A. Luther and V. J. Emery, Phys. Rev. Lett. **33**, 589 (1974).
- ⁴¹ I. E. Dzyaloshinskii and A. I. Larkin, Sov. Phys. JETP **34**, 422 (1972).
- ⁴² F. D. M. Haldane, Phys. Rev. B **25**, 4925 (1982).
- ⁴³ H. J. Schulz, G. Cuniberti, and P. Pieri, in *Field Theory for Low-Dimensional Condensed Matter Systems*, edited by G. Morandi, P. Sodano, A. Tagliacozzo, and V. Tognetti (Springer Verlag, New York, 2000), p. 9, cond-mat/9807366.
- ⁴⁴ V. J. Emery, A. Luther, and I. Peschel, Phys. Rev. B **13**, 1272 (1976).
- ⁴⁵ C. Bourbonnais and D. Jérôme, in *Advances in Synthetic Metals, Twenty Years of Progress in Science and Technology*, edited by P. Bernier, S. Lefrant, and G. Bidan (Elsevier, New York, 1999), pp. 206–261, arXiv:cond-mat/9903101.